J Am Oil Chem Soc (2007) 84:989–1000
DOI 10.1007/s11746-007-1139-0

ORIGINAL PAPER

Thermal and Textural Properties of Organogels Developed by Candelilla Wax in Safflower Oil

J. F. Toro-Vazquez · J. A. Morales-Rueda · E. Dibildox-Alvarado · M. Charó-Alonso · M. Alonzo-Macias · M. M. González-Chávez

Received: 4 May 2007 / Revised: 25 August 2007 / Accepted: 6 September 2007 / Published online: 13 October 2007

Abstract We investigated organogel formation in dispersions of CW in safflower oil (SFO). Candelilla wax (CW) has as its main component hentriacontane (78.9%), a *n*-alkane with self assembly properties in organic solvents (i.e., vegetable oils). Results showed that, independent of the cooling rate (i.e., 1 °C/min and 10 °C/min) and gel setting temperature (T_{set}), the CW organogels observed a thermoreversible behavior. This was evaluated by the behavior of thermal parameters that characterized organogel formation (gelation temperature, T_g; heat of gelation, ΔH_g) and melting (melting temperature, T_p; heat of melting, ΔH_M) after two heating-cooling cycles. For a given CW concentration (i.e., 0.5, 1.0, and 3%), the magnitude of ΔH_M and T_p and the structural organization of the organogel, depended on the cooling rate, the thermodynamic drive force for gelation, and the annealing process occurring at high T_{set} (i.e., 25 °C). At T_{set} of 25 °C the microplatelet units that formed the organogel aggregated as a function of storage time, a process that resulted in an increase in organogel hardness. In contrast, at T_{set} of 5 °C annealing occurred in a limited extent, but gels had higher solid fat content and microplatelet units of a smaller size than the gels obtained at 25 °C. The result was a three-dimensional network with greater hardness than the one obtained at 25 °C. The 3% CW organogels showed no phase separation up to 3 months at room temperature, with textures of potential use by the food industry.

Keywords Fat crystallization · Lipid chemistry · Lipid analysis · Thermal analysis · Lipid chemistry · Lipid analysis · Fats and oils

J. A. Morales-Rueda · M. Alonzo-Macias
Programa de Posgrado del Centro de la Republica (PROPAC),
Facultad de Quimica-DIPA,
Universidad Autonoma de Queretaro,
Queretaro, Mexico

J. F. Toro-Vazquez (✉) · J. A. Morales-Rueda · E. Dibildox-Alvarado · M. Charó-Alonso · M. Alonzo-Macias · M. M. González-Chávez
Facultad de Ciencias Quimicas-CIEP,
Universidad Autonoma de San Luis Potosi,
Av. Dr. Manuel Nava 6, Zona Universitaria,
San Luis Potosi 78210, Mexico
e-mail: toro@uaslp.mx

Introduction

Candelilla wax is a wax derived from the leaves of a small shrub native to northern Mexico and the southwestern United States, *Euphorbia cerifera* also known as *E. antisyphilitica*, from the family Euphorbiaceae. Candelilla wax (CW) is a worldwide recognized food additive approved by the FDA (under regulations 21CFR, 175.105, 175.320, 176.180) and, in accordance with regulation 184.1976, might be used in food with no limitation other than current good manufacturing practice. CW is used mainly as a glazing agent and binder for chewing gums. It also finds use in the cosmetic industry as a component of lip balms and lotion bars, and in the paint industry to make varnishes. Additionally, CW can be used as a substitute for carnauba wax and beeswax in different food systems. Reports on CW shows a composition of 49–50% *n*-alkanes with 29–33 carbons, 20–29% esters of high molecular weight, 12–14% alcohols and sterols, and 7–9% free acids [1, 2].

Vegetable oils, the most important edible lipids worldwide, lack the required functional properties to fit consumer demands for texture and stability in food products. As a result, partial hydrogenation of vegetable oils is

used to improve their plasticity and oxidation stability properties. Thus, in several countries partially hydrogenated vegetable oils are currently used in the formulation of functional shortenings, margarines, and confectionary coatings. Unfortunately, partially hydrogenation of vegetable oils results in the production of *trans* fatty acids that once ingested have a detrimental effect on cell membrane integrity, production of biologically active metabolites derived from essential fatty acids [3, 4], the high density to low density lipoproteins ratio [5], and their high consumption is a rate limiting factor for the Δ6-desaturase that converts the α-linoleic fatty acid into γ-linoleic [6] in the metabolic pathway of the ω-6 series. In consequence, health agencies such as the World Health Organization and the American Heart Association and the Dietary Guidelines 2005 issued recommendations to limit the *trans* fat intake. Within this framework the FDA set 1 January 2006 as the date by which all marketed foods must include *trans* fat concentration in the nutrition facts panel. These facts are influencing manufacturers to eliminate or reduce *trans* fats from their products [7]. Organogelation is a promising alternative that might be used to modify the physical properties of vegetable oils without the use of chemical modifications that result in the production of *trans*-fatty acids.

Organogels are bi-continuous colloidal systems that coexist as micro heterogeneous solid (i.e., gelator) and organic liquid phases [8]. In these systems the gelator is an organic molecule such as cholesteryl anthraquinone derivates [9], sterols [10], lecithin [11] and sorbitan monostearate [12], and the liquid phase is an organic solvent. In general, organogels formation is based in the spontaneous self-assembly of individual gelator molecules into three-dimensional networks of randomly entangled fiber-like structures. This three-dimensional network holds micro domains of the liquid in a non flowing state mainly through surface tension [13]. However, during the last years a different type of organogel has received attention, particularly because the gelators involved have low molecular weight and require only a small concentration (<2%) to achieve gelation. Compounds that fall in this category, generally know as low-molecular-mass organic gelator, are fatty acids [14] and *n*-alkanes [13]. CW has as its major component *n*-alkanes, opening the possibility of developing edible organogels through dispersions of CW in vegetable oil. Within this framework, the objective of this paper was to investigate the time–temperature conditions for the development of organogels using dispersions of CW in SFO high in triolein content (65–70% w/w). Additionally, we evaluated the thermal (i.e., heat of melting, melting temperature) and textural properties of CW organogels as a function of time at two storage temperatures (5 and 25 °C).

Materials and Methods

Vegetable Oil, CW, GC–MS, and HPLC Analysis

Safflower oil high in triolein (SFO) extracted from genetically modified seed was obtained from Coral International (San Luis Potosí, Mexico). Micronized high purity CW obtained from *E. cerifera* was supplied by Multiceras (Monterrey, Mexico). The SFO was analyzed for triacylglycerides (TAGs) by HPLC following the procedure described by Pérez-Martínez et al. [15]. The CW was analyzed by capillary GC in an Agilent Technology equipment model 6890N, coupled with a mass spectrometry detector model 5973N MSD. The column (HP-5; 30 m × 0.25 mm i.d.) had a matrix of 5% crosslinked phenyl–methyl siloxane (0.25 μm thickness). After sample injection (1 μL, split ratio 15:1), the initial temperature in the oven (100 °C) was held for 3 min, and then increased up to 340 °C (10 °C/min), holding this temperature for 23 min. The injection and ionizing ports were kept at 320 and 250 °C, respectively. After a solvent delay of 3 min, the mass spectra was scanned from 33 to 800 *m*/*z*. The identification of the components was made using the NIST 2 library (NIST, Gaithersburg, MD, USA).

Visual Appearance and Dynamic Gelation and Melting of Organogels

Different concentrations of CW were dispersed in SFO to achieve CW concentrations within 0 and 6% (wt/vol). The corresponding amount of CW was dispersed by heat (90 °C) and agitation in approximately 5 mL of SFO in a 10 mL volumetric flask. After dispersion the final volume was completed with SFO at room temperature. For preliminary studies 10 mL of these dispersions were stored at 5 and 25 °C in test tubes for visual appearance after 24 h of storage. The DSC equipment (TA Instruments Model 2920 coupled with a RCS cooling system; TA Instruments, New Castle, DE, USA), was calibrated as previously described [16] and was used for the dynamic gelation and melting studies. Samples of the CW dispersions (5–7 mg) were sealed in aluminum pans, heated at 90 °C for 20 min and then cooled to –80 °C at a rate of 10 °C/min. After 2 min at –80 °C the system was heated up to 90 °C at a rate of 5 °C/min. The temperature at the beginning of the gelation exotherm (T_g), the heat of gelation (ΔH_g), the temperature at the peak of the melting endotherm (T_p), and the heat of melting (ΔH_M) associated to the components of CW were calculated with the equipment software (TA-Instruments Universal Analysis 2000, v. 4.0). T_g and T_p were calculated using the first derivative of the heat flux. T_g was the temperature where the first derivative of the heat capacity of

the sample initially departed from the baseline. In contrast, T_p was the temperature where the first derivative of the heat capacity associated to the melting endotherm crossed the baseline. The ΔH_g and ΔH_M values corresponded to the areas under the gelation exotherm and melting endotherm, respectively. The corresponding thermal parameters for pure CW and SFO (i.e., vegetable oil with 0% CW) were also determined. Two independent determinations were done and the mean and standard deviation (sd) reported for statistical analysis.

Thermal Cycle Studies (Thermoreversible Gelation)

Two DSC thermal cycles, each consisting of cooling and heating stages, were applied to 0.5, 1.0, and 3% (wt/vol) CW dispersions in SFO. The process consisted of first heating (90 °C/20 min) samples of the dispersions (5–7 mg) sealed in aluminum pans, and then cooling the system at 1 °C/min or 10 °C/min until achieving a particular temperature (T_{set}). The organogels were allowed to set at this temperature for 30 min (i.e., isothermal gelation). Afterwards, the system was heated up to 90 °C (5 °C/min) and immediately cooled down again (i.e., second thermal cycle) at the same cooling rate (i.e., 1 °C/min or 10 °C/min) until achieving the same T_{set}. The organogels were developed isothermally at this T_{set} for 30 min. The second thermal cycle was concluded after heating the system again up to 90 °C (5 °C/min). From the cooling stage of each thermal cycle the T_g and ΔH_g values were calculated with the equipment software. In the same way, from the heating stage T_p and ΔH_M were also calculated. The T_{set}'s were selected based on the dynamic gelation thermograms for each of the CW dispersions (i.e., 0.5, 1.0, and 3% CW concentration in SFO) corresponding to the temperatures at the peak, the end, and 10 °C below the end of the gelation exotherm. Thus, for the 0.5 and 1.0% CW dispersions the corresponding T_{set}'s were 15, 5, and –5 °C, and for the 3.0% CW dispersion T_{set}'s were 30, 20 and 10 °C. The treatments evaluated resulted from the factorial combination of the thermal cycles applied, the different levels of T_{set}, and cooling rates investigated. The resulting treatments were distributed among aliquots of 0.5, 1.0, and 3% CW dispersions in a complete aleatory experiment design with two replicates. These CW concentrations were selected based on the visual appearance, apparent texture, and ΔH_g and ΔH_M values of 0–6% CW organogels developed and stored (24 h) at 25 °C. The statistical significance of the treatments' effect on the response variables (i.e., T_g, ΔH_g, T_p, and ΔH_M), was established through ANOVA and contrast among the treatment means using STATISTICA V 7.1 (StatSoft Inc., Tulsa, OK, USA).

Effect of Storage Time on the Solid Content, Thermal and Textural Properties of Organogels

After 20 min at 90 °C a given amount (20.0 mL) of 1 and 3% (wt/vol) CW dispersion in SFO, was dispensed into transparent plastic cups (height 3.9 cm, upper i.d. 3.5 cm, base i.d. 28 mm) and then stored at 5 or 25 °C (i.e., T_{set}). The solid content (SFC) of the CW dispersions was determined by pulsed NMR with a Minispec Bruker model mq20 (Brucker Analytik; Rheinstetten, Germany) in samples (3.5 mL) stored at the same temperatures. After achieving T_{set} (i.e., time zero) the ΔH_M, T_p, and the temperature at the end of the melting endotherm (T_e) were determined by DSC. Both, DSC analysis and SFC measurements were done as a function of time during the 10–14 days of storage at the corresponding T_{set}. At least two independent determinations ($n = 2$) were done in each case. The T_{set}'s for storage were selected based on the melting temperature (T_p) of the 1.0 and 3% CW organogels obtained after dynamic gelation. A T_{set} of 5 °C provided a high thermodynamic drive for gelation since this temperature was 30–40 °C below T_p for the 1 and 3% CW organogels. In contrast, a T_{set} of 25 °C provided a lower thermodynamic drive for gelation since this temperature was just 10–20 °C below the organogels' melting temperature. During storage the 0.5% CW organogels showed severe phase separation, particularly at 25 °C, affecting the reliability of the thermal and SFC measurements. Therefore, 0.5% CW organogels were not included in this experiment. On the other hand, force displacement curves of the organogels were obtained with a Texture Analyzer TA.XT plus (Stable Microsystems, Surrey, UK) using a flat stainless steel cylindrical probe (20 mm diameter). A temperature control chamber was used to maintain the sample temperature (i.e., T_{set}) during texture measurements. Thus, the organogels in the cups were penetrated up to 10 mm from the surface at a speed of 1 mm/s, and then the probe was pulled out from the sample at the same speed. Using the equipment software (Texture Exponent 32; Stable Microsystems) the force displacement curves were obtained by plotting the force applied (grams-force) to the sample as a function of penetration depth. Analysis of the force displacement curves with the equipment software provided the gel strength or strength at rupture (*g*-force), the maximum force applied (*g*-force), and the work of shear (g/mm). The correspondence of these parameters to the force displacement curves obtained is shown in Fig. 1. For a given T_{set} and storage time at least five independent determinations were done ($n = 5$). To determine the time the system achieved T_{set}, thermocouples were inserted in the plastic cups filled with CW dispersions. The time at which the system achieved T_{set} was considered time zero of storage. The temperature in the

plastic cups decreased in an exponential way providing a non-constant cooling rate. Thus, for a T_{set} = 25 °C decreasing the temperature from 90 °C down to 60 °C showed a cooling rate of 6.0 °C/min, between 60 and 40 °C the cooling rate was 2.0 °C/min, and between 40 °C and T_{set} the cooling rate was 1.0 °C/min. For a T_{set} = 5 °C decreasing the temperature from 90 °C down to 50 °C, we observed a cooling rate of 6.0 °C /min, between 50 and 25 °C the cooling rate was 2.0 °C/min, and between 25 °C and T_{set} the cooling rate was 1.0 °C/min.

Polarized Light Microscopy

Polarized light microphotographs (PLM) of the 1 and 3% CW organogels were obtained using a polarized light microscope (Olympus BX51; Olympus Optical Co., Ltd., Tokyo, Japan) equipped with a color video camera (KP-D50; Hitachi Digital, Tokyo, Japan) and a platina (TP94; Linkam Scientific Instruments, Ltd., Surrey, England) connected to a temperature control station (LTS 350; Linkam Scientific Instruments, Ltd.) and a liquid nitrogen tank. To guarantee a uniform sample thickness, a drop of the melted sample was gently smeared over a preheated glass microscope slide (90 °C) using another glass slide at a 45° angle. The slide with the sample was placed in the platina and after 20 min at 90 °C the system was cooled to T_{set} with the temperature control station (Linksys32-version 1.3.1; Linkam Scientific Instruments Ltd. Waterfield, UK) programed with a variable cooling rate as a function of the temperature. The program was set up according to the corresponding cooling profile previously determined for CW dispersions (see "Effect of storage time on the solid content, thermal and textural properties of organogels"). PLMs of the organogels were obtained as a function of storage time once T_{set} was attained. To avoid water condensation over the glass slides stored at 5 °C, these were placed inside a hermetic plastic box with silica gel.

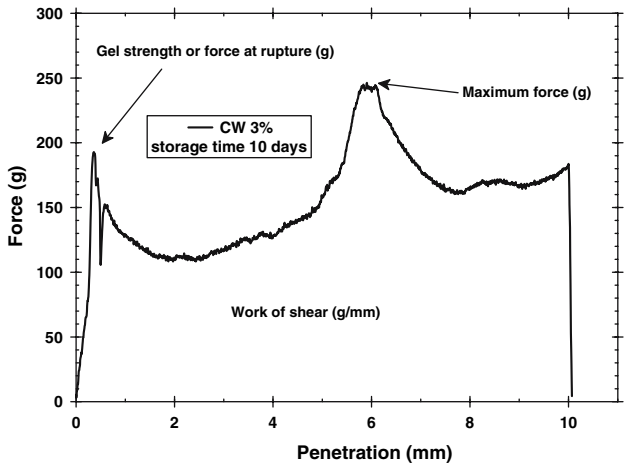

Fig. 1 Characteristic force displacement curve showing the textural parameters measured in the CW organogels

Results and Discussion

The results of the CW analysis showed the main characteristic of CW [1, 2, 17], i.e., a high proportion of *n*-alkanes with 29–33 carbons (Table 1). The main component of CW was hentriacontane (78.9%), a *n*-alkane with the molecular formula $CH_3(CH_2)_{29}CH_3$, molecular weight of 436.85, melting point (99.5% purity) of 67.05 °C, and ΔH_M of 73.3 kJ/mol [18]. The CW thermograms showed just one major exotherm with a T_g of 76.58 °C (sd = 0.68 °C), two temperature peaks at 59 and 53 °C, and ΔH_g of 147.35 J/g (sd = 1.91 J/g) (Fig. 2a). The corresponding heating thermogram showed just one endotherm with a melting temperature (T_p) of 64.42 °C (sd = 0.23 °C) and a ΔH_M of 149.75 J/g (sd = 1.20 J/g) (Fig. 2a). The T_p of CW was close to the melting temperature reported for 99.5% pure hentriacontane (i.e., 67.05 °C) [18]. However, the ΔH_M calculated per unit mass of hentriacontane (82.9 kJ/mol) was greater than the ΔH_M reported for 99.5% hentriacontane (i.e., 73.3 kJ/mol) [18]. It is important to point out that besides triterpenoids, other *n*-alkanes such as nonacosane and tritriacontane (Table 1), were present as minor components in CW. These compounds might develop a mixed molecular packing with hentriacontane during cooling. Such mixed structures might explain the two temperature peaks present in the CW exotherm (Fig. 2a) and the greater ΔH_M in comparison with the one for pure hentriacontane. Based on these results the phase transitions observed in the CW's thermograms were associated with the phase behavior of hentriacontane.

The thermograms of CW dispersions in SFO showed two peaks (Fig. 2b). The peak present below 0 °C in both the cooling and heating thermograms (Fig. 2b) was associated to the crystallization and melting of TAGs from

Table 1 GC–MS composition of CW

Name	Condensed formula	%[a]
Nonacosane	$C_{29}H_{60}$	4.16 ± 0.11
Hentriacontane	$C_{31}H_{64}$	78.86 ± 0.11
Tritriacontane	$C_{33}H_{68}$	8.01 ± 0.15
Alcohols of penta-cyclic triterpenoids[b]	$C_{30}H_{49}OH$	7.38 ± 0.08
Unidentified	–	1.60 ± 0.07

[a] Mean and standard deviation of two determinations (n = 2). Values reported as a percentage of the total area

[b] Any or all of the following isomers: germanicol, lupeol or Hop-22(29)-en-3, β-ol

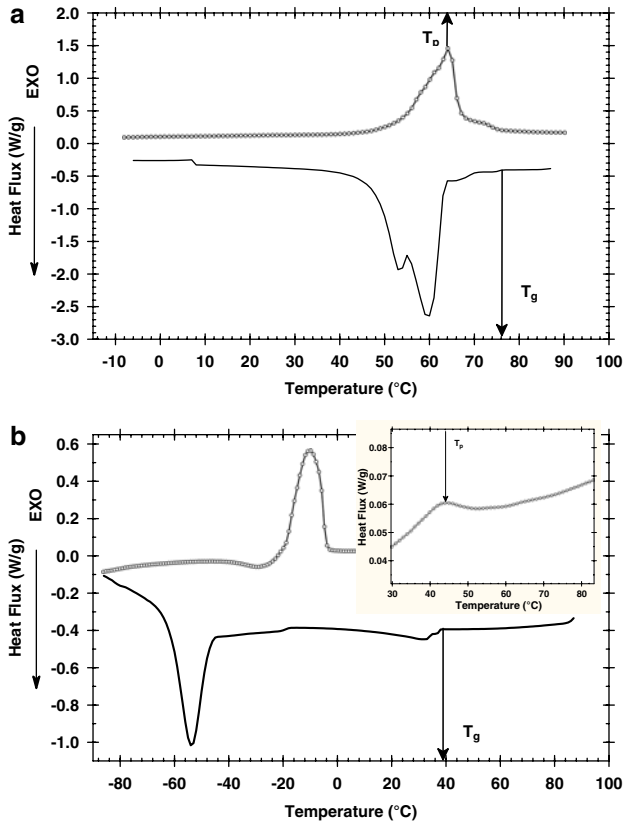

Fig. 2 Cooling (*solid line*) and heating (*dotted line*) thermograms for CW (**a**) and a 3% CW dispersion in SFO (**b**). The insert is the enlarged section between 30 and 80 °C for the heating thermogram, showing the endotherm for the CW dispersion. T_p and T_g are defined in the text

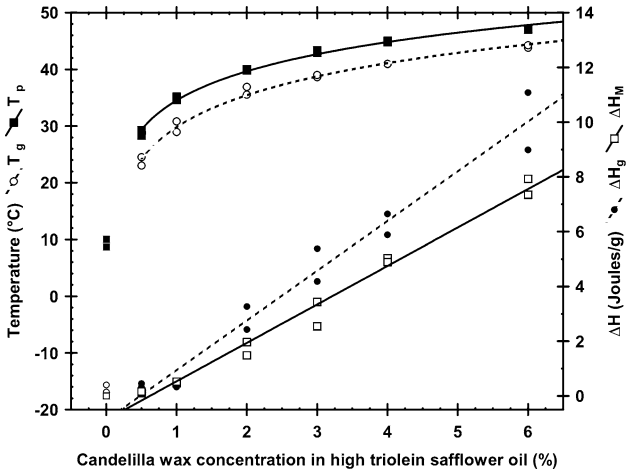

Fig. 3 Behavior of the thermal parameters that characterized organogel development (T_g, ΔH_g) and melting (T_p and ΔH_M) as a function of CW concentration in SFO. T_g, ΔH_g, T_p, and ΔH_M are defined in the text

SFO. This, since the major TAG present in SFO was OOO with 63.32% (sd = 0.06), followed by 17.25% LnOO (sd = 0.27), 8.86% POO (sd = 0.12), 2.85% StOO (sd = 0.07), and 2.59% LnLnO (sd = 0.06). The other peak, always present above 0 °C in both the cooling and heating thermograms, was associated with the gelation (Fig. 2b) and melting (see the insert of Fig. 2b) of CW components, mainly hentriacontane. Within the interval of CW concentration investigated (i.e., 0–6% CW) the thermal parameters that described this peak (e.g., T_g, ΔH_g, T_p, and ΔH_M) increased as CW concentration increased (Fig. 3). The T_g and T_p of CW dispersions showed similar behavior as the one observed by the T_g of several *n*-alkanes when dissolved in different organic solvents [8, 13], i.e., a steady logarithmic increase as a function of CW concentration followed by a plateau. Regarding the hysteresis observed by ΔH_g and ΔH_M (Fig. 3), this phenomenon was associated, as Abdallah et al. [8] pointed out, with the inclusion of the gelator's heat of dissolution within the ΔH_M value. The hysteresis effect was more important as the concentration of the gelator molecules increased in the system (i.e., as CW concentration increased) and more mass of gel was developed. It is important to point out that fitting lines for T_g, ΔH_g, T_p, and ΔH_M showed in Fig. 3, did not consider the thermal parameters for the 0% CW dispersion.

After 24 h of storage at 5 °C, CW dispersion developed gels at all concentrations investigated. At all CW concentrations the gels remained at the bottom of the test tubes even after turning the tubes upside down. Gels were clear at 0.5% CW and as CW concentration increased gels' opacity increased, particularly at CW concentrations ≥2% (data not shown). In contrast, the CW dispersions stored at 25 °C for 24 h developed a clear sol-type system at 0.5% CW and a translucent gel at 1% CW that slowly flowed after test tubes' inversion. As CW concentration increased to values ≥2% non transparent to opaque gels were obtained (Fig. 4) that did not flow upon inverting the test tubes. The ΔH_g values at CW concentrations ≥2% showed a significant increase ($P < 0.01$) in comparison with the values for the 0.5 and 1% CW organogels (Fig. 3). These results showed that, independent of the storage temperature, dispersions of CW developed a well-structured three-dimensional network at concentrations ≥2%. However, at CW concentrations lower than 2%, the gelator molecules of CW required a storage temperature lower than 25 °C (i.e., 5 °C) to organization in a three dimensional network that physically entrapped the SFO. Based on these results three CW concentrations were selected to perform the thermoreversible gelation studies. Two of these CW concentrations had a gelation process temperature dependent and were lower than 2% (i.e., 0.5 and 1.0%), while the other had a gelation process temperature independent and was higher than 2% (i.e., 3%). These CW concentrations ought to provide different levels of structural organization of the gelator molecules in the solvent phase (i.e., SFO).

Thermal Properties of CW Organogels

The thermal cycles applied at the CW dispersions (0.5, 1.0 and 3%) did not have a significant effect on T_g, ΔH_g (i.e., organogel formation), T_p, and ΔH_M (i.e., organogel melting) at any of the cooling rates (i.e., 1 °C/min and 10 °C/min) investigated. Therefore, under the experimental conditions studied, organogels developed by CW in SFO showed a thermoreversible behavior. As an example, Fig. 5 shows the cooling and heating thermograms for the two thermal cycles applied at a cooling rate of 1 °C/min to the 3% CW system. Similar results were obtained at 10 °C/min and for the 1% CW system (results not shown). Within this framework, we studied the cooling rate and T_{set} effect on gelation and melting of CW organogels independent of the thermal cycle applied. The results showed that at each of the CW concentrations investigated T_{set} did not have a significant effect on T_g (data not shown). However, both T_g and ΔH_g were higher at 1 °C/min than at 10 °C/min and the higher the CW concentration the higher T_g and ΔH_g (Fig. 6a, b). Then, at 1 °C/min gelator molecules present in CW (i.e., hentriacontane) achieved the required structural alignment for gel development at a higher T_g than at 10 °C/min ($P < 0.001$; Fig. 6a). This observation applied for each of the CW concentration investigated. These results might be explained considering that during the cooling stage, the thermodynamic driving force for gel formation (e.g., the difference between the temperature of the system and the temperature at which molecules achieve the molecular alignment for gel formation), changed faster as the cooling rate increased. Then, at 10 °C/min gelator molecules (i.e., hentriacontane) had less time to organize than at 1 °C/min, requiring a lower temperature (i.e., lower T_g) to achieve the molecular packing for organogel formation. Independent of the cooling rate and at each CW concentrations T_{set} showed an inverse linear relationship with ΔH_g ($P < 0.01$; Fig. 6c). These results were expected since, as described in the experimental section, the T_{set}'s evaluated corresponded to temperatures at the peak, end, and 10 °C below the end of the gelation exotherm.

The parameters associated to organogels' melting, particularly ΔH_M, were considered as measurements directly associated with the structural order of the gelator molecules within the assembly units that form the organogel. Within this framework and in contrast to the parameters that characterized the gelling process, T_p (data not shown) and ΔH_M (Fig. 7) showed a significant dependence on both, T_{set} and cooling rate ($P < 0.01$). The T_{set} and cooling rate effect on T_p and ΔH_M was different at each CW concentration (Fig. 7). Nevertheless, we observed a general behavior since at low T_{set}'s higher T_p and ΔH_M (i.e., higher level of molecular structure) were obtained than at high T_{set}'s. This behavior was more evident at 1 °C/min than at 10 °C/min. As previously established gel formation required a lower T_g at 10 °C/min than at 1 °C/min (Fig. 6a). In consequence, during the isothermal stage at a given T_{set} organogels had a lower thermodynamic driving force (i.e., $T_g - T_{set}$) at 10 °C/min than at 1 °C/min. Therefore, organogels developed at the higher cooling rate had a lower level of molecular organization in their assembly units (i.e., lower ΔH_M) than organogels developed at 1 °C/min. However, under certain time-temperature conditions (i.e., 1% CW, 10 °C/min, T_{set} = 15 °C; Fig. 6b), particularly at high T_{set}'s, we observed deviations from this behavior. This might be explained considering that the other *n*-alkanes present in CW as minor components (Table 1), might develop a mixed molecular packing with hentriacontane with the subsequent effect on ΔH_M and T_p. Nevertheless, annealing within the

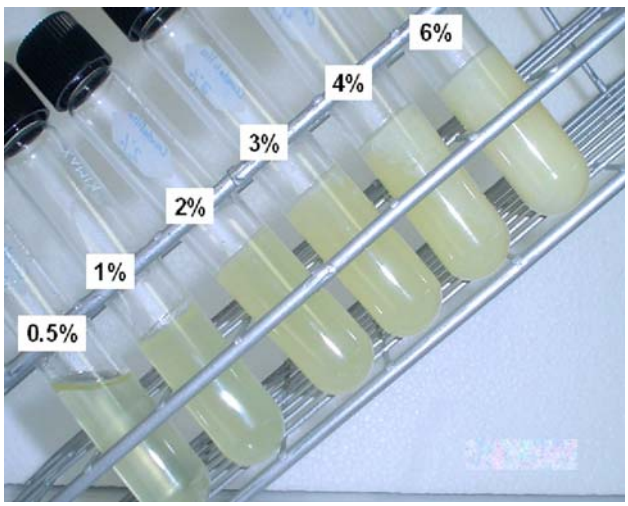

Fig. 4 Visual appearance of organogels developed at 25 °C as a function of CW concentrations in SFO

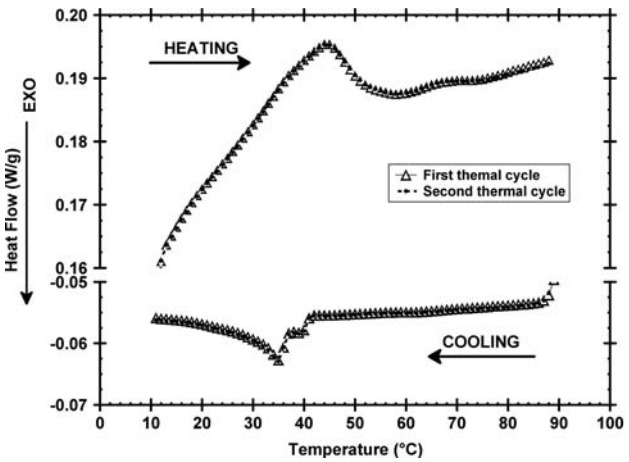

Fig. 5 Cooling and heating thermograms for the two thermal cycles applied to a 3% CW system using a cooling rate of 1 °C/min

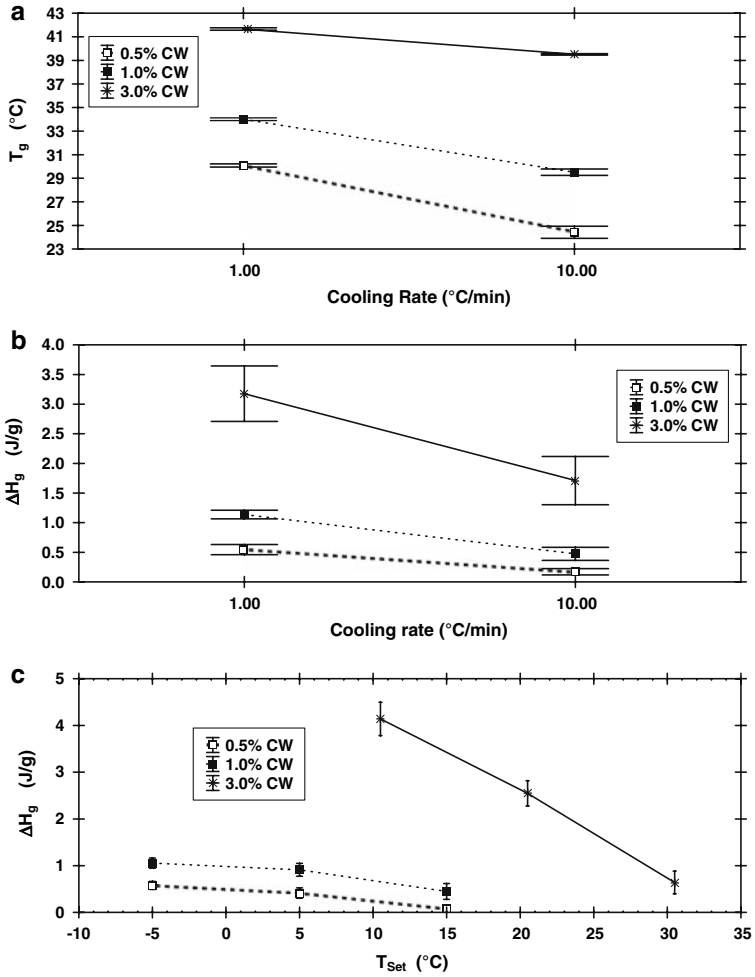

Fig. 6 Effect of cooling rate on T_g (**a**) and ΔH_g (**b**) in organogels developed at different concentrations of CW. Effect of T_{set} on ΔH_g in organogels developed at different CW concentrations (**c**). T_g, ΔH_g, and T_{set} are defined in the text

assembly units of the organogel structure might be considered as an additional explanation. Such molecular reorganization might take place during the isothermal stage as long as T_{set} was close or above the end of the gelation exotherm (i.e., 15 °C at 0.5 and 1% CW, and 30 °C at 3% CW). Then, for a given CW concentration, the structural organization of the organogel and therefore, ΔH_M and T_p, depended on the cooling rate, the thermodynamic drive force for gelation during the isothermal stage, and probably an annealing process occurring at high T_{set}. The gelation mechanism of carbamates provided similar observations [19].

Organogels Stored at T_{set}'s of 5 and 25 °C

The ΔH_M measurements for the 1% CW organogels (Fig. 8a) showed higher variation as a function of storage time than the 3% CW organogels (Fig. 8b) at both 5 and 25 °C. Such variation was the result of a phase separation experienced by the 1% CW organogels after 7–8 days of storage, particularly at T_{set} of 25 °C. In contrast, the 3% CW organogels were stable and no phase separation was observed even after 45 days of storage at either 5 or 25 °C. Despite the variation observed in the ΔH_M values for the 1% CW organogels, independent of storage time, this parameter was always higher in the systems stored at 25 °C than in the ones stored at 5 °C ($P < 0.05$; Fig. 8). For the 3% CW organogels, ΔH_M increased steadily as a function of storage time until achieving a plateau. Such plateau values were greater at a T_{set} of 25 °C than at 5 °C (Fig. 8b). The ΔH_M behavior could not be associated to changes in the SFC during storage, mainly because the SFC achieved by the organogels right after attaining T_{set} remained constant during the whole period of storage in all systems evaluated. The corresponding mean SFC for the 1 and 3% CW organogels during the 10–14 days of storage at 5 and 25 °C are shown in Table 2. Evidently, independent of the CW concentration, the organogels' SFC was always higher at 5 °C than at 25 °C ($P < 0.01$). Regarding the behavior of T_p and T_e, both values also remained constant under the time-temperature conditions investigated (Table 2). Nevertheless, independent of the CW concentration, T_e was higher in the organogels stored at 25 °C than in the ones

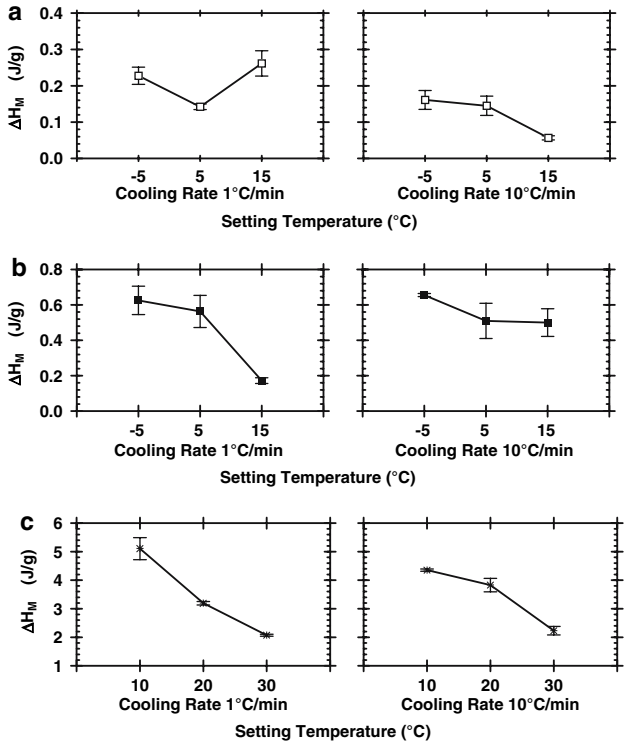

Fig. 7 Effect of cooling rate and setting temperature on ΔH_M for organogels developed at 0.5% (**a**), 1% (**b**), and 3% (**c**) CW concentration in SFO. ΔH_M is defined in the text

stored at 5 °C ($P < 0.001$; Table 2). T_p for the 1% CW organogels observed a similar behavior than T_e, but in the 3% CW organogels T_p was statistically the same at both 5 and 25 °C (Table 2).

We explained the behavior of the organogels' thermal parameters under the following considerations. The sol-gel transition during organogel formation, always resulted in the organization of microcrystalline structures that develop a three-dimensional network that physically restrains the liquid phase and finally sets up the gel structure. The shape and size of microcrystalline structures vary with the chemical characteristics of the gelator molecule (i.e., fatty acid, sterols, phospholipids, *n*-alkanes) [10, 11, 14], but also might be affected by annealing. Although annealing has been extensively studied in starches [20], hydrogels [21], and liquid crystals [22], there is no agreement in the molecular mechanism involved during this process. Nevertheless, it is generally accepted that after molecules attain a three-dimensional organization, an appropriate combination of time and temperature results in additional ordering of the three-dimensional molecular structure (i.e., annealing or perfection of the crystalline regions) and/or ordering of amorphous regions. In polymers with crystalline structures such as starch, annealing is more effective at temperatures just below the melting temperature. Over time, this process generally results in structures with higher crystallinity than the ones showed by non annealed systems. This as measured by ΔH_M, the melting temperature, and X-ray diffraction [20, 21] of the system. Although no X-ray studies were done on the CW organogels, the behavior of T_e and T_p, and particularly the ΔH_M increase as a function of time in the systems stored at 25 °C, suggested the occurrence of annealing. As previously mentioned annealing might take place during the isothermal stage as long as T_{set} is close or above the end of the gelation exotherm (i.e., 15 °C at 1% CW and 30 °C at 3% CW). Then, the organogels stored at 25 °C resulted in structures with higher melting parameters than the ones showed by organogels stored at 5 °C. However, additional investigations are required to determine whether the annealing process is associated with an increase in the domain size within the organogel assembly units or to a polymorphic transformation.

Regarding the texture measurements the 3% CW organogels showed, at both T_{set}'s, the force displacement curve show in Fig. 1. The force displacement curves for the 1% CW organogels stored at 5 °C and 25 °C did not show the characteristic peak associated to gel strength. This indicated that, independent of T_{set}, the 1% CW organogels offered limited or no resistance to probe penetration during texture measurements, i.e., the surface of 1% CW organogels was softer than the 3% CW organogels. Therefore, the subsequent comparisons between the texture of the 1 and 3% CW organogels were limited just to the work of shear and the maximum force. These parameters were considered as relative measurements of organogels' hardness and at the two CW concentrations investigated both showed the same behavior as a function of storage time. Thus, the relative hardness measured as the work of shear, increased during the 1–2 days of organogels' storage (Table 2). This, except the1% CW organogels stored at 25 °C (Table 2). After 1–2 days of storage the relative hardness achieved a value that remained constant during the rest of the storage (Table 2). Additionally, for the same T_{set} the relative hardness was always higher in the 3% CW organogels than in the 1% CW organogels ($P < 0.01$). These results showed that hardness of the 1 and 3% CW organogels increased as a function of storage time in a similar way as ΔH_M. However, while hardness had greater values in the organogels stored at 5 °C than in the ones stored at 25 °C ($P < 0.01$), ΔH_M observed the opposite behavior (Fig. 8). As previously discussed the annealing phenomenon might be associated to the ΔH_M behavior in the CW organogels. However, additional factors have to be considered to explain the organogels' textural behavior.

In food systems the microstructural organization of the solid phase and its interaction with the liquid phase determines most of their rheology and texture. This is particularly evident in systems where crystallization of

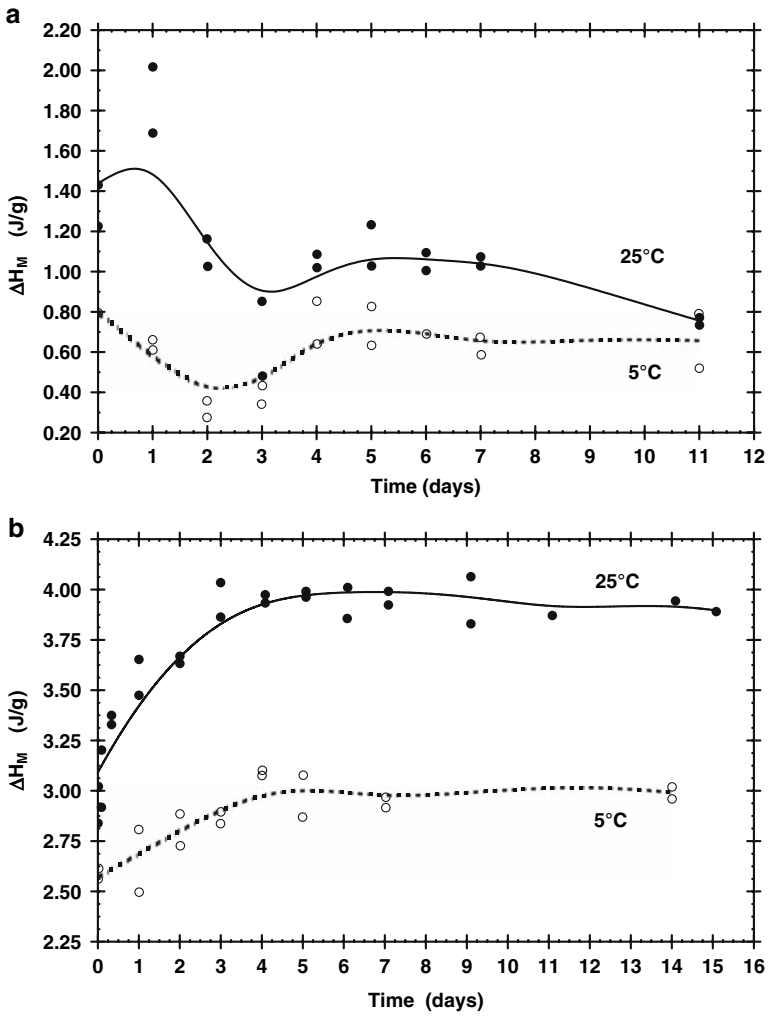

Fig. 8 Heat of melting (ΔH_M) as a function of storage time at two T_{set} (5 and 25 °C) for organogels developed at 1% (**a**) and 3% (**c**) CW concentration in SFO. ΔH_M is defined in the text

TAGs plays an important role, i.e., chocolate, butter, margarine. In such systems a higher SFC is generally associated to higher rheological and textural values [23, 24]. Within this context the higher SFC present in the 3% CW organogels in comparison with the 1% CW (Table 2), particularly at T_{set} of 5 °C, might explain in part the higher hardness observed by the 3% CW systems in comparison with the 1% CW systems. However, the increase in the organogels' hardness as a function of storage time could not be associated with an increase in SFC. As previously indicated, for a given T_{set} and CW concentration, the SFC of the organogels remained constant during storage (Table 2). Then, structural characteristics of the organogels had to be considered to explain the increase in the organogels' hardness. Within this framework, Dr. Marangoni's group [24–26] established that the rheology of colloidal aggregates networks depends, in addition to SFC, on the average size and shape of the solid particles, the solid–liquid surface energy, the particle–particle interactions, and the three-dimensional organization of the solid phase (i.e., the fractal dimension). In particular, the smaller the size of the primary particles that form a three-dimensional network, the higher the rheology of the system [24–26]. The PLMs of the 1 and 3% CW organogels stored at both T_{set}'s investigated showed a structure formed by microcrystalline particles of colloidal dimensions that aggregated as a function of storage time (Fig. 9). At both CW concentrations, the microcrystalline structures that formed the organogels at T_{set} of 5 °C (Fig. 10a, c) were smaller than the microstructures formed at T_{set} of 25 °C (Fig. 10b, d). Additionally, PLMs showed that during storage at 25 °C aggregation of the microcrystalline structures occurred at a higher extent (Figs. 9d, h, 10b, d) than at 5 °C (Figs. 9b, f, 10a, c). To associate these results with the microstructural characteristics of the CW organogels we used the model established by Dr. Weiss' group [27] for the microcrystalline structures (i.e., microplatelet units) of hexatriacontane organogels. Hentriacontane differs from hexatriacontane just in the length of the hydrocarbon chain (i.e., C31 vs. C36). Thus, the self

Table 2 Relative hardness (measured as the work of shear, g/mm), solid fat content (SFC), melting temperature at the peak (T_p) and end (T_e) of the endotherm for organogels of CW developed and stored at two temperatures (T_{set})

T_{set}	1% CW					3% CW				
	Work of shear 0 days[a] (g/mm)	Work of shear 1–10 days[a] (g/mm)	SFC (%)	T_p (°C)	T_e (°C)	Work of shear 0 days[a] (g/mm)	Work of shear 2–14 days[a] (g/mm)	SFC (%)	T_p (°C)	T_e (°C)
5 °C	370.78[b] (23.16)	438.08[c] (44.61)	0.90[d] (0.14)	35.90[d] (0.21)	49.00[d] (0.18)	2415.46[b] (201.14)	2742.98[c] (232.64)	2.57[d] (0.14)	44.83[d] (0.22)	59.46[d] (0.20)
25 °C	37.18[b] (4.30)	37.18[b] (4.30)	0.59[e] (0.13)	39.48[e] (0.21)	51.13[e] (0.18)	1455.54[b] (102.44)	1542.15[c] (119.72)	2.11[e] (0.12)	44.00[d] (0.17)	69.90[e] (0.15)

At each CW concentration and T_{set}, the value of hardness corresponded to the storage period indicated. The SFC, T_p, and T_e are the mean values for the storage period (i.e., 10 or 14 days) at the corresponding T_{set}

[a] For a given storage time the values are the mean and standard deviations of five independent measurements ($n = 5$)

[b, c] For the same CW concentration and T_{set}, values with different letter were statistically different ($P < 0.05$)

[d, e] For the same CW concentration values with different letter were statistically different ($P < 0.01$)

assembly organization of the microplatelet units and the microplatelet three-dimensional structure of hentriacontane organogels ought to be similar to the one established for hexatriacontane organogels [27]. In hexatriacontane organogels the microplatelet units are formed by parallel alignment (i.e., lamellar alignment) of *n*-alkane molecules maintained by van der Waals forces. Liquid molecules of the *n*-alkane do not occupy interlamellar sites, except at the junction zones that link the microplatelet units into the three-dimensional network [27]. Such junction zones quite probably establish the organogel strength and therefore, organogels' texture. Within this framework and considering the calorimetry and textural results for CW organogels, we established the following conclusions. During organogel storage at 25 °C, the gelator molecules within the microplatelet units and probably at the junction zones, reorganize its molecular packing achieving a higher level of structural organization. As a result, the ΔH_M of the CW organogels increased. During this process aggregation among the microplatelet units also occurred, developing a three-dimensional organization with an open structure that physically entrapped the liquid phase (Figs. 9d, 10b for the 1% CW; Figs. 9h, 10d for 3% CW). The result was an increase in the organogel's texture as a function of storage time. In contrast, at T_{set} of 5 °C annealing occurred in a limited extent, and therefore the increase in ΔH_M during storage was smaller than at 25 °C. Although the formation of junction zones among microplatelet units also occurred at 5 °C (to develop the organogel's three-dimensional organization), at this T_{set} the microplatelets were of smaller size than at 25 °C. Additionally, the SFC was higher at 5 °C than at 25 °C (Table 2). The result was a three-dimensional network of microplatelet units with a more dense organization (Figs. 9b, f, 10a, c) than the network formed at 25 °C (Figs. 9d, h, 10b, d). Therefore, the greater hardness showed by organogels formed at T_{set} of 5 °C in comparison with the ones formed at 25 °C (Table 2), was associated with their greater SFC but also with the smaller microplatelet unit size that formed the organogel's three-dimensional network. Viscosity of the liquid phase in the CW organogels (i.e., SFO) was greater at 5 °C (i.e., 177.1 cps with a sd = 1.7) than at 25 °C (i.e., 64.6 cps with a sd = 2.6) ($P < 0.001$). Then, it is plausible to assume that molecular diffusion of gelator molecules and therefore the growth and aggregation of microcrystalline structures were lower in organogels stored at 5 °C than in the ones stored at 25 °C.

Previous research had shown the organogelation of saturated fatty acids, fatty alcohols, wax esters, and dicarboxylic acids [28] in vegetable oils. However, this research only described a possible structure–function relationship associated to the gelling properties of such compounds in vegetable oils. The results obtained here

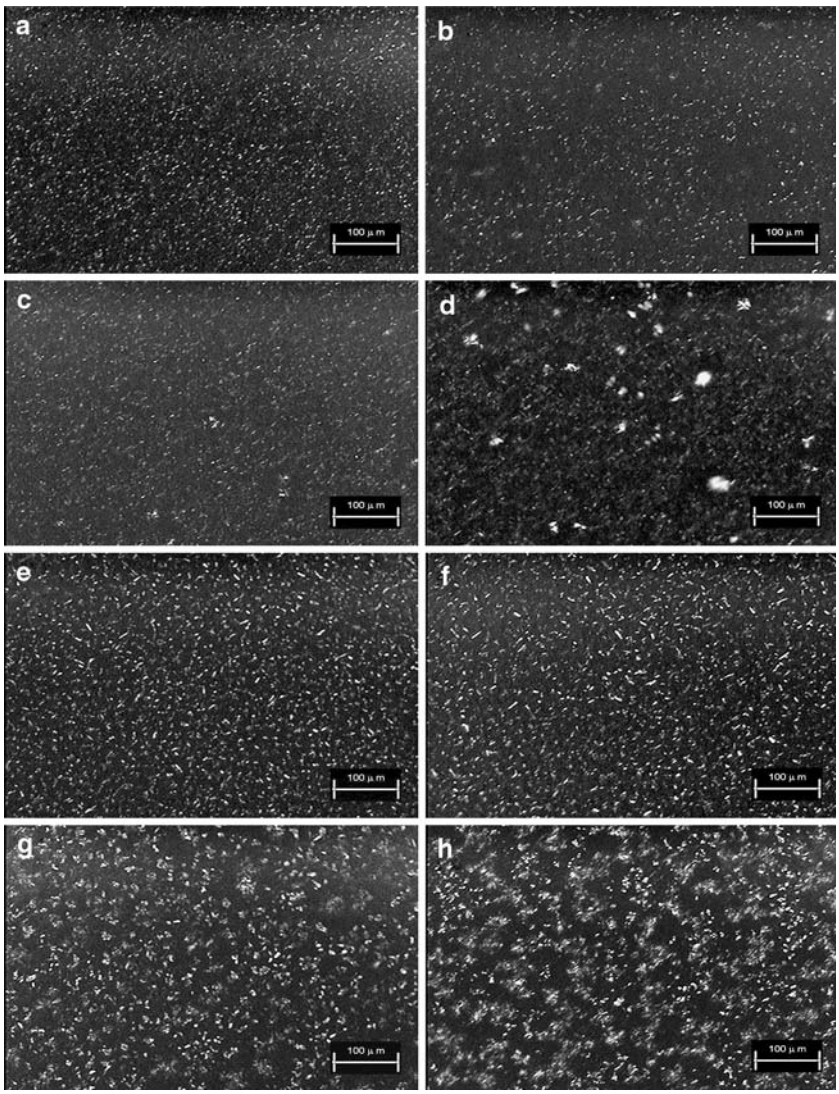

Fig. 9 Polarized light microphotographs (20× magnification) of CW organogels at different days of storage at T_{set} of 5 and 25 °C. T_{set} of 5 °C, 1% CW organogels at 0 days (**a**) and 11 days (**b**) of storage. The same conditions but T_{set} of 25 °C after 0 days (**c**) and 11 days (**d**) of storage. T_{set} of 5 °C, 3% CW organogels at 0 days (**e**) and 14 days (**f**) of storage. The same conditions but T_{set} of 25 °C after 0 days (**g**) and 14 days (**h**) of storage

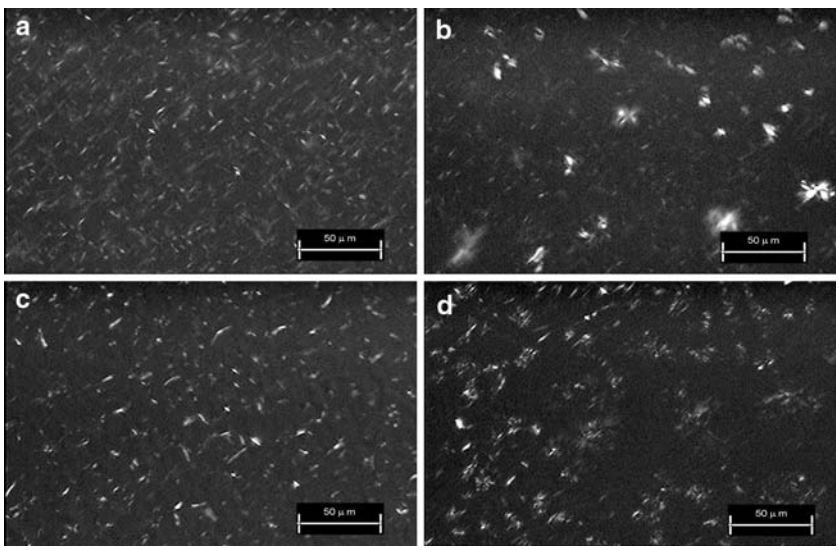

Fig. 10 Polarized light microphotographs (50× magnification) of CW organogels at 7 days of storage at T_{set} of 5 °C (**a**, **c**) and 25 °C (**b**, **d**). 1% CW (**a**, **b**) and 3% CW (**c**, **d**)

showed that we might modify the physical appearance of SFO high in triolein through organogelation with CW and without the use of *trans*-fats. In fact, thermoreversible edible organogels might be obtained applying time-temperature conditions to CW dispersions in SFO. The 3% CW organogels showed a phase separation stability at least up to 3 months, providing textures with potential use for the food industry.

Acknowledgments The investigation was supported by grant #48273-Z from CONACYT. The technical support from Concepcion Maza-Moheno and Elizabeth Garcia-Leos is greatly appreciated.

References

1. Grant DL (2005) Candelilla wax, first draft. WHO food additive series 30, http://www.inchem.org/documents/jecfa/jecmono/v30je12.htm
2. Instituto de la Candelilla (2004) http://www.candelilla.org/es/propiedades.htm
3. Mensink RP (2005) Metabolic and health effects of isomeric fatty acids. Curr Opin Lipidol 16:27–30
4. Stender S, Dyerberg J (2004) Influence of *trans* fatty acids on health. Ann Nutr Metab 48:61–66
5. Ascherio A., Stampfer MJ, and Willett WC (1999) Trans fatty acids and coronary heart disease, http://www.hsph.harvard.edu/reviews/transfats.pdf
6. Manku MS, Horrobin DF, Morse N, Kyte V, Jenkins K, Wright S, Burton JL (1982) Reduced level of prostaglandin precursors in the blood of atopic patients: defective Δ-6-desaturase function as a biochemical base for atopy. Prostaglandins Leukot Med 9:615–628
7. Kodali RD, List GR (Eds.) (2005) *Trans* fats alternatives. AOCS, Champaign
8. Abdallah DJ, Lu L, Weiss RG (1999) Thermoreversible organogels from alkane gelators with one heteroatom. Chem Mater 11:2907–2911
9. Ostuni E, Kamaras P, Weiss RG (1996) Novel X-ray method for in situ determination of gelator strand structure: polymorphism of cholesteryl anthraquinone-2-carboxylate. Angew Chem Int Ed Engl 35:1324–1326
10. Bot A, Agterof WGM (2006) Structuring of edible oils by mixtures of γ-oryzanol with β-sitosterol or related phytosterols. J Am Oil Chem Soc 83:513–521
11. Kumar R, Katare OP (2005) Lecithin organogels as a potential phospholipid-structured system for topical drug delivery: a review. AAPS PharmSciTech 6:E298–E310
12. Murdan S, Gregoriadis G, Florence AT (2000) Novel sorbitan monostearate organogels. J Pharm Sci 88:608–614
13. Abdallah DJ, Weiss RG (2000) *n*-Alkanes gel *n*-alkanes (an many other organic liquids). Langmuir 16:352–355
14. Wright AJ, Marangoni AG (2007) Time, temperature, and concentration dependence of ricinelaidic acid-canola oil organogelation. J Am Oil Chem Soc 84:3–9
15. Pérez-Martínez D, Alvarez-Salas C, Morales-Rueda J, Toro-Vazquez JF, Charó-Alonso M, Dibildox-Alvarado E (2005) The effect of supercooling on crystallization of cocoa butter–vegetable oil blends. J Am Oil Chem Soc 82:627–632
16. Toro-Vazquez JF, Dibildox-Alvarado E, Charó-Alonso MA, Herrera-Coronado V, Gómez-Aldapa CA (2002) The Avrami index and the fractal dimension in vegetable oil crystallization. J Am Oil Chem Soc 79:855–866
17. LipidBank (2006). http://www.lipidbank.jp/cgi-bin/detail.cgi?id=WWA1101
18. INFOTHERM (2006). http://www.fiz-chemie.de/infotherm/servlet/infothermSerch
19. Huang X, Raghavan SR, Terech P, Weiss RG (2006) Distinct kinetic pathways generate organogels networks with contrasting fractality and thixotropic properties. J Am Chem Soc 128:15341–15352
20. Hoover R, Vasanthan T (1994) The effect of annealing on the physicochemical properties of wheat, oat, potato and lentil starches. J Food Biochem 17:303–325
21. Köhler K, Förster G, Hauser A, Dobner B, Heiser UF, Ziethe F, Richter W, Steiniger F, Drechsler M, Stettin H, Blume A (2004) Temperature-dependent behavior of a symmetric long-chain bolaamphiphile with phosphocholine headgroups in water: from hydrogel to nanoparticles. J Am Chem Soc 126: 16804–16813
22. Leclair S, Baillargeon P, Skouta R, Gauthier D, Zhao Y, Dory YL (2004) Micrometer-sized hexagonal tubes self-assembled by a cyclic peptide in a liquid crystal. Angew Chem Int Ed 43:349–353
23. Campos R, Narine SS, Marangoni AG (2002) Effect of cooling rate on the structure and mechanical properties of milk fat and lard. Food Res Intern 35:971–981
24. Marangoni AG, Rogers MA (2003) Structural basis for the yield stress in plastic disperse systems. Appl Phys Lett 82:3239–3241
25. Narine SS, Marangoni AG (1999) Mechanical and structural model of fractal networks of fat crystals at low deformations. Phys Rev E 60:6991–7000
26. Marangoni AG (2000) Elasticity of high-volume fraction fractal aggregate networks: a thermodynamic approach. Physical Rev Lett B 62:13951–13955
27. Abdallah DJ, A., S.A., Sirchio, Weiss RG (2000) Hexatriacontane organogels. The first determination of the conformation and molecular packing of a low-molecular-mass organogelator in Its gelled state. Langmuir 16:7558–7561
28. Daniel J, Rajasekharan R (2003) Organogelation of plant oils and hydrocarbons by long-chain saturated FA, fatty alcohols, wax esters, and dicarboxylic acids. J Am Chem Soc 80:417–421